24th COBEM - 2017

24th ABCM International Congress of Mechanical Engineering
December 3-8, 2017, Curitiba, PR, Brazil

COBEM-2017-2921
SYNTHESIS AND CHARACTERIZATION OF CNT-O_2 THIN FILMS AS DOUBLE LAYER CAPACITOR ELECTRODE

Marina Borgert Moraes
Gilmar Patrocinio Thim
Instituto Tecnológico de Aeronáutica - ITA
marinaborgert@msn.com

Abstract. *As the search for renewable energy sources rises, there's also a growing need for more efficient energy storage devices, and researches on this field become more and more important. The use of innovative electrode materials seeks to improve energy density and lifetime span of such devices. In this context, nanomaterials, especially carbon nanotubes, appear very promising. This work focuses on the study of vertically aligned carbon nanotubes, treated by oxygen plasma, for utilization as an electrochemical capacitor electrode. Characterization analysis of the samples consisted of Raman spectroscopy and scanning electron microscopy images. To evaluate electric energy storage capacity and behavior, cyclic voltammetry, electrochemical impedance spectroscopy and charge/discharge routines were employed. Samples presented specific capacitance up to 192.71 F/g for voltammetry evaluation and a value of 201.23 F/g was obtained through discharge curves. For some samples, it was noted the contribution of pseudo-capacitance. From the Nyquist plot, it was possible to estimate electrolyte resistance, charge transfer resistance and double layer capacitance.*

Keywords: *carbon nanotubes, thin films, electrical double layer capacitors, energy storage.*

1. INTRODUCTION

Climatic changes and the decrease in fossil fuels availability have compelled researches for renewable and sustainable energies sources. As a result, it can be observed an increase in sun and wind energy production as well as the development of electric or hybrid vehicles. Since it is not possible to control such energy sources to produce on demand, there is a necessity to store this energy; it is also necessary to improve autonomy and performance of hybrid and electric vehicles (Etacheri *et al.*, 2011). Consequently, energy storage systems become more relevant to society, ensuring the autonomy of vehicles and portable devices (Simon and Gogotsi, 2008).

On the vanguard of electric energy storage systems we have batteries and electrochemical capacitors. Electrochemical capacitors, also known as double layer capacitors or supercapacitors, store energy physically in an electrical double layer at the interface between a large surface area electrode and an electrolyte medium by electrostatic interactions. This kind of storage comes from the ionic and electronic charge separation at this interface. These supercapacitors are unique devices that have high power density and long life cycle. However, it is important to keep improving their capacity and performance to attend the most demanding requirements of future systems through the development of new materials and the advances in the comprehension of electrochemical interfaces at nanometric levels.

Carbon nanotubes (CNT) have been studied in electrochemical devices due to their outstanding intrinsic properties, such as electrical conductivity, chemical and mechanical stability and high surface area, and have been used on supercapacitors (Li and Chen, 2017), electrochemical sensors (Punbusayakul, 2012), etc. Their electrochemical performance depends on the orientation and chemical functionalization of the tubes; it has been shown that electrodes based on vertically aligned CNT present better electrocatalytic activity than those with randomly oriented tubes (Moraes *et al.*, 2013) due to the presence of many CNT containing their free tips per area unit, which in vertically aligned carbon nanotubes based electrodes increases electron transfer rate.

Though CNT are promising materials for development of supercapacitors, there are a few issues that may pose serious drawbacks for its performance. One issue is the lowering of the contact resistance between CNTs and collector electrodes in the supercapacitor, which can be achieved by mixing nanotubes with conductive binders and coating collector electrodes. But this process drastically modifies nanotube electrode properties, leading to undesirable

capacitive performance. This difficulty can be avoided by devising techniques for direct growth of CNT on the current collector.

In this paper we have reported the synthesis and performance of oxygen functionalized CNT grown directly over Ti alloy substrates. Vertically aligned CNT grown on the Ti metallic surface provide high conductivity due to the exceptional electrical contact between the CNT film and the current collector, and the oxygen functionalization enhances the interface of the double layer in aqueous solution electrolyte.

2. EXPERIMENTAL

CNT films were grown over a 1 cm^2 Ti-6Al-4V alloy plate, with 0.05 cm thickness. These plates were previously sanded and polished, and cleaned with isopropyl alcohol in a bath ultrasound for 10 minutes; after cleaning, the plates were heated to 600 °C to form a thin layer of TiN/TiO_2 on its surface to act as a diffusion barrier and prevent the catalyst from penetrating the plate. The nickel catalyst was deposited over the diffusion barrier by electron-beam evaporation as a thin film of 10 nm.

The plates were each deposited inside the Microwave assisted Chemical Vapor Deposition (MWCVD) reactor, as shown in Fig. 1. The reactor has an anodized aluminum chamber, and its pressure was monitored by a Barocel sensor. The gas flow was controlled by a MKS-247C mass flow controller. There are quartz windows at the sample holder level (for observation) and there is a tungsten resistance under the sample holder to warm it. Temperature was monitored by thermocouple located in an orifice at the center of the sample holder.

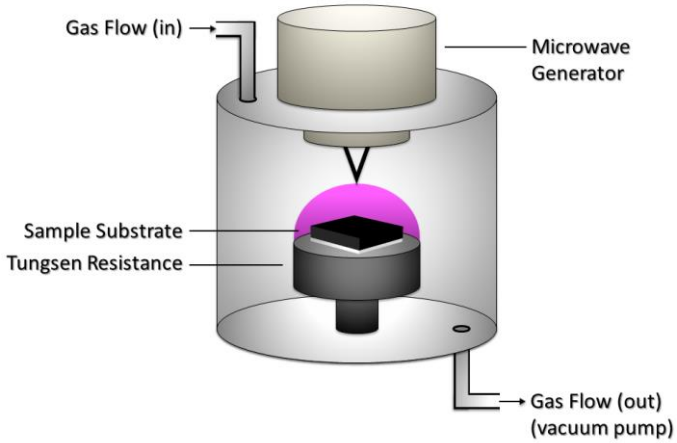

Figure 1. Schematic of MWCVD reactor and sample.

Synthesis of CNT involved two stages. At the first, the samples were heated up to 300 °C and then submitted to nitrogen (N_2, 10 sccm) and hydrogen (H_2, 90 sccm) plasma at 6 x 10^3 Pa for five minutes, increasing temperatures up to 800 °C. This step is necessary to create nano-islands of the metallic catalyst on the sample surface, so they can nucleate the nanotubes later. At the second stage, methane flow (CH_4, 14 sccm) was initiated as a carbon source for 2 minutes, when the CNT film grew vertically aligned.

After CNT growth, samples were functionalized by oxygen in a pulsed-DC plasma reactor with an oxygen (O_2) flow rate of 1 sccm, at a pressure of 80 mTorr, tension of 700 V and frequency of 20 kHz, to achieve a super-hydrophilic aspect, which is crucial for its electrochemical application.

CNT morphology and structure was observed by SEM images and Raman spectroscopy. SEM images were obtained in a JEOL JSM 5310 VPI. Raman spectra was acquired in a Renishaw 2000 system with excitation by Ar ion laser (514.5 nm) in backscattering geometry and 100 s of exposure time. The samples containing the CNT-O_2 film were immobilized on a copper plate using conductive silver paste, and used as working electrode. A geometric area of 0.317 cm^2 was employed in all electrochemistry assays. The specific capacitance, cyclic voltammetry, electrochemical impedance spectroscopy and constant current charge/discharge under galvanostatic conditions experiments were performed in H_2SO_4 0,5 M at 25 °C using an Autolab PGSTAT-30 (Metrohm) potentiostat/galvanostat controlled with the GPES 4.9 software. All electrochemical experiments were carried out in a 100 mL Metrohm three-electrode cell, with an Ag/AgCl reference electrode and a Pt foil as auxiliary electrode. The mass of CNT film was calculated by weight difference measured in an analytical electronic microscale (Mettler MT5).

3. RESULTS AND DISCUSSION

Figure 2a shows SEM images of the CNT vertically aligned film as grown. It is very homogeneous and the tubes length can be estimated as 25 µm. In Fig. 2b it is shown a sample after 10 minutes of interaction with water; during this time, water has permeated the film surface and has penetrated the film through the empty spaces. After its evaporation, the tubes have grouped together forming irregular micropatterns and breaking the film alignment, so it is clear that the as-grown film could not interact properly with aqueous solutions as electrolyte medium, because low wettability means there will be high impedance for charge transfer (Silva *et al*., 2014).

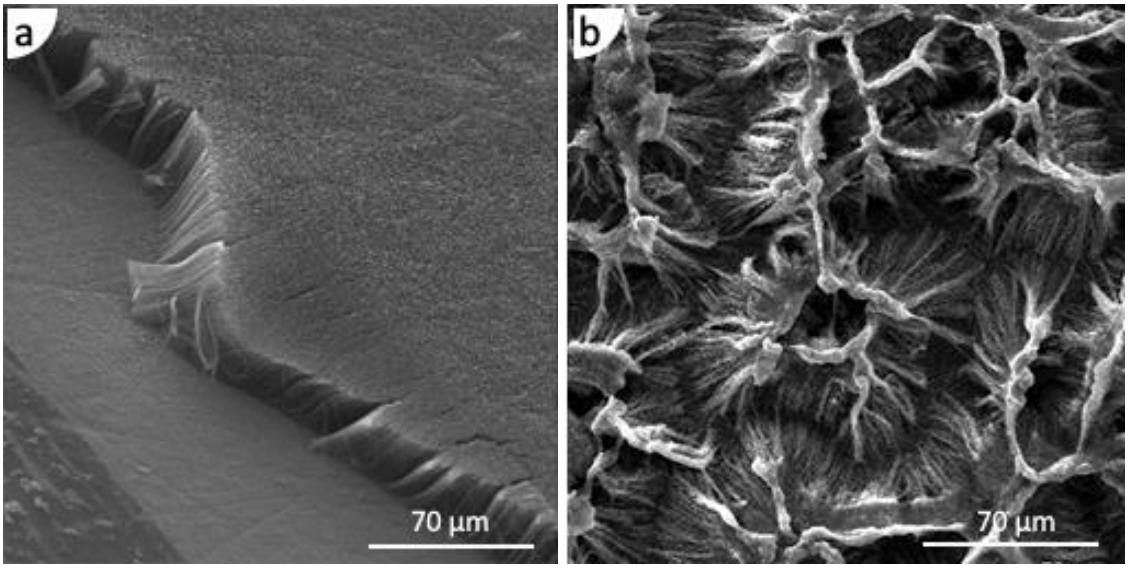

Figure 2. SEM images of (a) homogeneous CNT film as-grown on titanium alloy (approximated thickness of 25 µm); (b) hydrophobicity effect observed on CNT film.

To study the structure changes on the CNT films after O_2 plasma functionalization, Raman spectroscopy was used. Figure 3 presents the first order spectra for three distinct samples: CNT as-grown, CNT-O_2 treated by 1 minute, and CNT-O_2 treated by 2 minutes. The deconvolutions were performed using Lorentzian shapes for the D, G and G' bands d for band and peak identification (Zanin *et al*., 2014). In Fig. 3a, we can confirm the presence of CNT by D and G bands positioned at 1354.97 cm^{-1} and 1580.44 cm^{-1} respectively. G band is characteristic of graphitic layers and corresponds to the tangential vibration of carbon atoms; it is slightly asymmetric, appearing close to the frequency of graphite (Costa *et al*., 2008). D band in carbon materials is usually attributed to some disorder characteristic, generated by the effect of finite particle size on the structure (crystalline network distortion). For CNT, changes in D band can indicate structural alterations in the walls due to the introduction of different chemical species. According to Osswald *et al*. (2005), the presence of D band is not necessarily an intrinsic characteristic of CNT, since it can be originated from amorphous carbon in the sample, but for the specific case of multi-walled CNT the defects on tubes walls generate a signal much stronger than for single and double-walled CNT. Due to the MWCVD technique used to synthesize CNT, it is estimated that the samples did not contain considerable amounts of amorphous carbon due to the abundant quantity of hydrogen available inside the reactor chamber. The intensity of D band can be attributed to the closed caps of the tubes and catalyst particles enclosed on the film surface, since the analysis was performed on top of the CNT film.

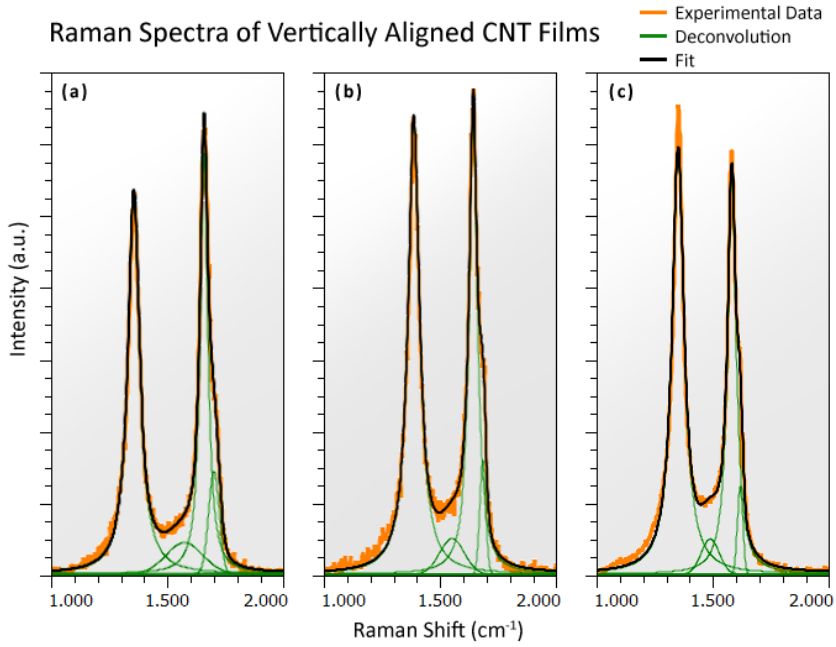

Figure 3. First order Raman spectra for CNT: (a) as-grown; (b) treated by O_2 plasm for 1 minute; (c) treated by O_2 plasm for 2 minutes.

In Fig. 3b and 3c it becomes clear that O_2 plasma functionalization has changed the surface of CNT films, adding highly polar oxygen-containing groups which, as result, turned the wettability of the films to superhydrophilic. There was no significative change in the positions of D and G bands, as shown in Table 1. I_D/I_G ratio is usually seen as an indicative of the level of functionalization in CNT (Rao *et al*., 2000). The small increase in I_D/I_G ratio can be justified by the opening of the tubes caps (tips) and the aggregation of oxygen functional groups on it positively influencing the D band. Changes in I_D/I_G ratio were possibly minimized by the removal of metallic catalyst particles once present on the film surface, and can also be due to different film densities in the analyzed area.

Table 1. Raman spectra data extracted from deconvolution.

Samples	**D band (cm^{-1})**	**G band (cm^{-1})**	**FWHM (D)**	**FWHM (G)**	**I_D/I_G**
CNT	1354,97	1580,44	61,52	44,20	0,86
CNT – O_2 [1 min]	1354,99	1580,37	47,34	31,07	0,91
CNT – O_2 [2 min]	1350,01	1581,27	44,79	28,91	1,05

According to Ramos (2011), changes observed on relative intensity and full width at half maximum (FWHM) are related to symmetry breaking of the ordered hexagonal structure of the nanotubes walls. This symmetry breaking causes the alteration of hybridizing sp^2 bonds to sp^3, and may be a consequence of the oxidative process of functionalization. Along with changes in wettability, the insertion of oxygenated groups has another purpose: according to Holloway *et al*. (2008), CNT with oxidized tips (very defective) present higher electron transfer rate than CNT with none or few defects, indicating that electroactive sites are located on the CNT tips (region with most defects and free chemical bonds).

To characterize the electrochemical behavior, various parameters were tested. The reference electrode was positioned as close as possible to the working electrode, to reduce the resistance effect from the aqueous solution as well as to keep the same distance between the electrodes in the cell (Zoski, 2007). For CNT films, specific capacitance can be estimated from cyclic voltammograms according to Eq. (1):

$$C_e = \frac{\mathrm{I}}{v.m} \tag{1}$$

Where I is the current equivalent to the applied tension, *v* is the scan speed and *m* is the total mass of the working electrode, as reported by Shah *et al*. (2009) and Niu *et al*. (2011). Other authors propose that to better evaluate the specific capacitance by cyclic voltammograms it is necessary to consider that the cathodic and anodic voltammetric charging do not present the same behavior, as shown in Eq. (2), since the curves do not present mirrored symmetry (Chen *et al.*, 2010).

$$C_e = \frac{\int_{E_1}^{E_2} \mathrm{I(E)\,dE}}{2(E_2 - E_1)v.m} \tag{2}$$

Where $\int_{E_1}^{E_2} I(E)dE$ is the total voltammetric charge obtained by integration of positive and negative cycles of the scan; $(E_2 - E_1)$ is the amplitude of potential window; *v* is the scan speed expressed in $mV.s^{-1}$ (typically between 1 and 200 $mV.s^{-1}$) and *m* is the total mass of the working electrode. Wei *et al*. (2008) have analyzed the capacitance from cyclic voltammograms in terms of electrode area, as shown in Eq. (3):

$$C_e = \frac{\mathrm{I}}{v.A} \tag{3}$$

Where I is the capacitive current, *v* is the scan speed and *A* is the working electrode area.
Figures 4 and 5 show the cyclic voltammograms of different CNT-O_2 samples at different scan rates.

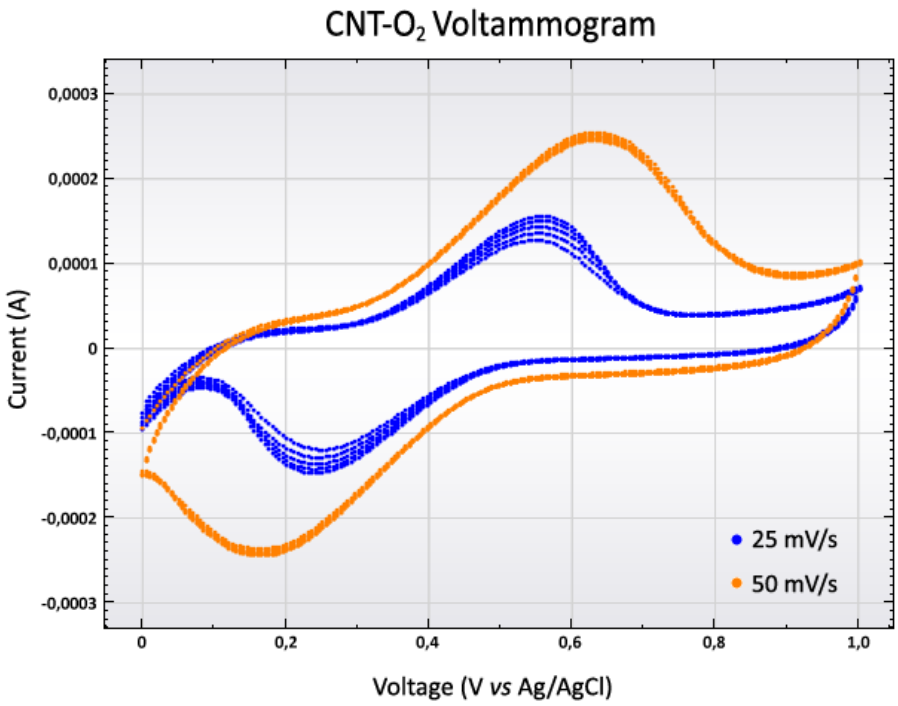

Figure 4. Cyclic voltammogram at different speeds for CNT-O_2 electrode.

According to Eq. (1), specific capacitance was calculated as 164.40 $F.g^{-1}$ for 25 $mV.s^{-1}$ scan speed; and as 109.09 $F.g^{-1}$ for 50 $mV.s^{-1}$ scan speed. Specific capacitance was also calculated according to Eq. (2), resulting in 49.92 $F.g^{-1}$ for 25 $mV.s^{-1}$ scan speed and 25.07 $F.g^{-1}$ for 50 $mV.s^{-1}$ scan speed. Capacitance per area was estimated using Eq. (3) as 1.76 $mF.cm^{-2}$ for 25 $mV.s^{-1}$ scan speed; and as 1.17 $mF.cm^{-2}$ for 50 $mV.s^{-1}$ scan speed.

The electrical current registered by the working electrode may originate from the occurrence of quick and reversible redox reactions on the electroactive species in the aqueous solution, which in turn generate a Faradaic current. This Faradaic current depends on kinetics, diffusion transport of electroactive species and the charge transfer reactions at the

electrode interface (Bird, 2010). The capacitive double layer charging may contribute to the Faradaic current, and it increases along with scan speed.

When capacitors have redox reactions at the surface of its material, it produces what is known as pseudocapacitive behavior. Specific pseudocapacitance generally exceeds the capacitance of carbon materials, but due to the use of redox reactions these systems suffer from lack of stability during their life cycle. The presence of pseudocapacitance is denoted by the redox peaks and is related to Faradaic processes and not to the double layer capacitance. Therefore, the capacitance values for this sample have received a contribution of pseudocapacitance and the real double layer capacitance is probably smaller than estimated by these calculations. Kim *et al.* (2010) have reported that pseudocapacitive behavior can be caused by oxygen groups produced by oxidative treatments, which induce Faradaic processes.

According to several authors (Niu *et al*., 2011; Chen *et al*., 2002; Cui *et al*., 2011), pseudocapacitance can be partly attributed to residual metallic particles from the catalyst, and also to the distribution of nanotubes in the film; it can contribute greatly to specific capacitance. However, as the CNT films were treated with oxygen plasma, we believe that this process caused the opening of the tubes tips and has removed any residue of the nickel catalyst on the film surface.

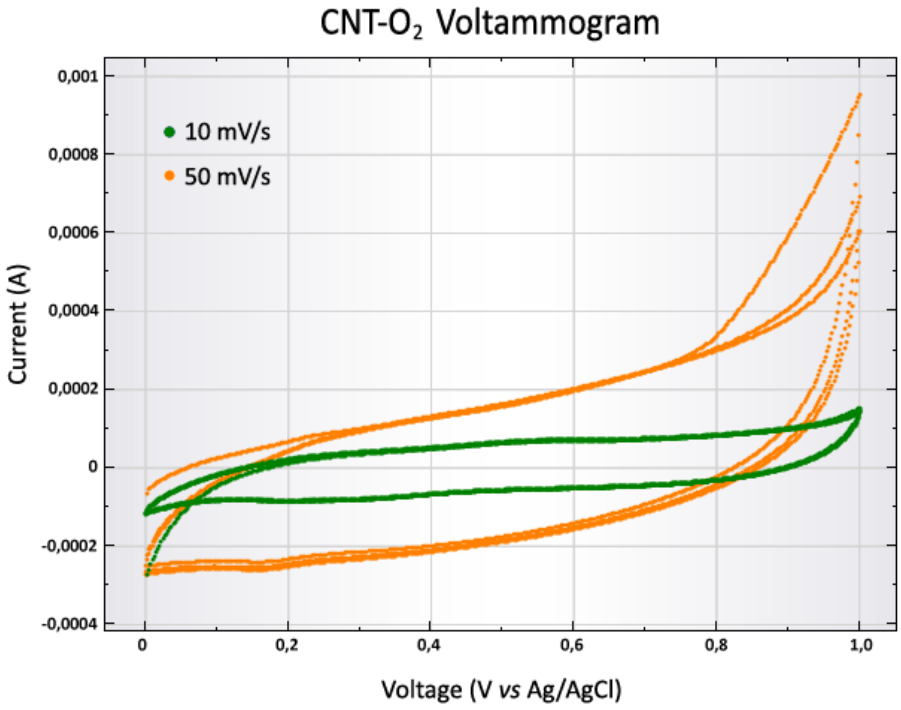

Figure 5. Cyclic voltammogram at different speeds for CNT-O_2 electrode.

Figure 5 voltammograms present a featureless, "quasi-rectangular" shape, which is typical of interfacial double layer charging in a non-Faradaic process and are most likely a result of CNT distribution (Chen *et al*., 2002). Cyclic voltammetry measurements from 10 mV.s-1 to 50 mV.s^{-1} showed that the specific capacitance values are not constant for low scan rates, which indicates that the system wasn't under equilibrium conditions. According to Eq. (1), specific capacitance was calculated as 192.71 F.g^{-1} for 10 mV.s^{-1} scan speed; and as 96.20 F.g^{-1} for 50 mV.s^{-1} scan speed. Specific capacitance was also calculated according to Eq. (2), resulting in 150.16 F.g^{-1} for 10 mV.s^{-1} scan speed and 50.44 F.g^{-1} for 50 mV.s^{-1} scan speed. Capacitance per area was estimated using Eq. (3) as 2.07 mF.cm^{-2} for 10 mV.s^{-1} scan speed; and as 1.03 mF.cm^{-2} for 50 mV.s^{-1} scan speed. A comparison of these estimations is shown in Table 2.

Table 2. Comparison of specific capacitances obtained by the equations presented by Shah *et al.* (2009) and Niu *et al*. (2011); Chen *et al.* (2010); and Wei *et al*. (2008).

Samples	**Scan speed ($mV.s^{-1}$)**	**Capacitance by Shah and Niu (F/g)**	**Capacitance by Chen (F/g)**	**Capacitance by Wei ($mF.cm^{-2}$)**
$CNT\text{-}O_2$ (Fig. 4)	25	164.40	49.92	1.76
	50	109.09	25.07	1.17
$CNT\text{-}O_2$ (Fig. 5)	10	192.71	150.16	2.07
	50	96.20	50.44	1.03

It was observed that specific capacitance of the $CNT\text{-}O_2$ films decreases with the increase in scan speed. This is partly a limitation of the technique, in which the time span between each potential step doesn't allow the capacitor to fully charge before the execution of the next step. In this sense, the lower scan speeds results are more accurate.

One of the main limitations of cyclic voltammetry regarding sensitivity is the capacitive current, which is a component of the background or residual current. Faradaic current also contributes to the background current, and can occur due to process related to several factors, such as impurities in the electrolyte or other reagents used, and as oxygen dissolved in the cell medium (Aleixo, 2003).

Since CNT present electronical properties sensitive to structural variations (length, diameter, helicity), the voltammogram is a mean of very close peaks representing the electron transfer for each tube (Kim *et al.*, 2010). The thickness of the double layer is usually determined by electrolyte concentration and by the ions size, up to a few angstroms (Simon and Burke, 2008). Specific capacitance obtained with acid or alkaline aqueous solutions is generally higher than that obtained with organic electrolytes, although the latter are able to withstand a greater operating potential (up to approximately 3 V), so specific applications can benefit from both kinds of electrolytes: supercapacitors using aqueous solutions are appropriated for pulsed applications, while supercapacitors using non-aqueous systems are indicated to attend high energy demands (Guittet, 2011).

Another way to evaluate the specific capacitance is from calculations based on charge and discharge cycles. Galvanostatic cycles were performed using chronopotentiometric technique, within the limit between 0 and 1 V with applied current density of 100 $\mu A.cm^{-2}$ in open circuit potential. Figure 6 presents charge and discharge curves for a $CNT\text{-}O_2$ electrode *versus* Ag/AgCl in H_2SO_4 (0.5 M).

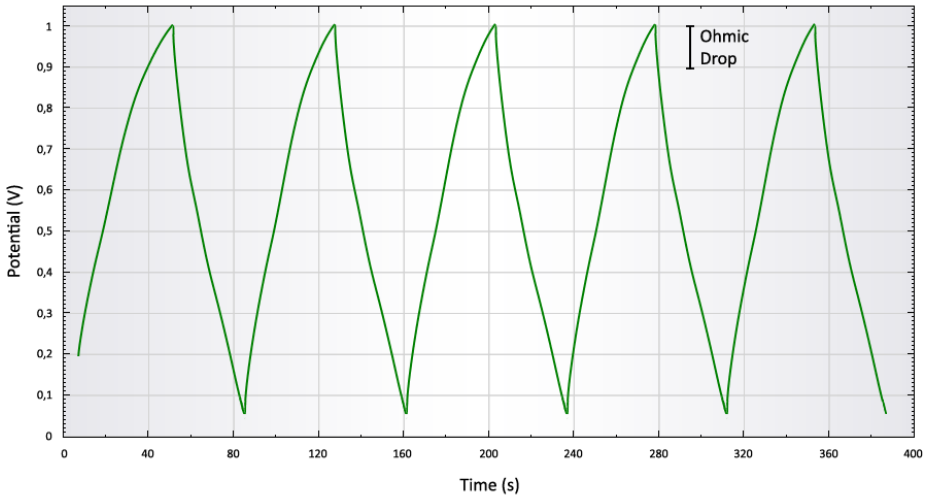

Figure 6. Charge and discharge curves for $CNT\text{-}O_2$ electrode *versus* Ag/AgCl in H_2SO_4 (0.5 M), with current density 100 $\mu A/cm^2$.

The main characteristic of these curves is its non-linear and non-triangular shape, with a noticeable ohmic drop at the beginning of the discharge cycles. The ohmic drop indicate resistive effects in the electrode, which are responsible for cell heating (Joule effect), leading to energy loss that can't be converted in work. If intense, this heating can cause degradation of the electrode materials. It can also increase the electrolyte vapor pressure resulting in leakage or

explosion of the battery or capacitor. The ohmic drop may suggest that current density is too elevated for the electrolyte ionic conductivity (Oliveira and Bertazzoli, 2011).

According to Guittet (2011), charge and discharge curves should have triangular shape for ideal capacitive behavior (constant ratio between potential range and time). it is more appropriate to estimate the capacitance with Eq. (4):

$$C_e = \frac{\mathrm{I}\Delta \mathrm{t}^2}{2m\int_0^{\Delta t} V dt} \tag{4}$$

Where I is the applied current, Δt is the discharge cycle time, m is the total mass of the working electrode and $\int_0^{\Delta t} V dt$ is the potential range obtained by discharge cycle integration (Guittet, 2011). Using Eq. (4) the specific capacitance was calculated as 201.23 $F.g^{-1}$. Shah *et al*. (2009) and Niu *et al*. (2011) have used the following Eq. (5) to estimate specific capacitance:

$$C_e = \frac{\mathrm{I}\Delta \mathrm{t}}{(dV/dt).m} \tag{5}$$

Where I is the discharge current, Δt is the discharge cycle time, (dV/dt) is the slope of discharge curve and *m* is the total mass of the working electrode. According to Eq. (5), specific capacitance was estimated as 127.36 $F.g^{-1}$. Table 3 presents a comparison between this research and other supercapacitors based on CNT grown on metallic substrates found in literature, that were characterized in aqueous electrolytes. Concentrations of aqueous solutions were disregarded and whenever available, the scan speed closest to 10 $mV.s^{-1}$ was chosen.

Table 3. Comparison of specific capacitances found in literature.

Reference	**Voltammetry ($F.g^{-1}$)**	**Charge and Discharge ($F.g^{-1}$)**
This work	192,71	201,23
Chen *et al*., 2002	146	115,7
Gao *et al*., 2008	83	-
Kim *et al*., 2012	160	-
Niu *et al*, 2011	34	35
Ramos, 2011	-	915
Shah *et al*., 2009	21,57	14,6
Yoon *et al*., 2004	207,3	-

From Table 3 it is clear that highly different results are found in literature, and the methodologies to determine a material's performance as an electrode for supercapacitors are far from standardized. In addition, each methodology can contribute significantly to the estimated capacitance.

Electrochemical impedance spectroscopy was used to investigate the behavior of CNT-O_2 film. Figure 7 shows the Nyquist plot for a CNT-O_2 film functionalized for 1 minute.

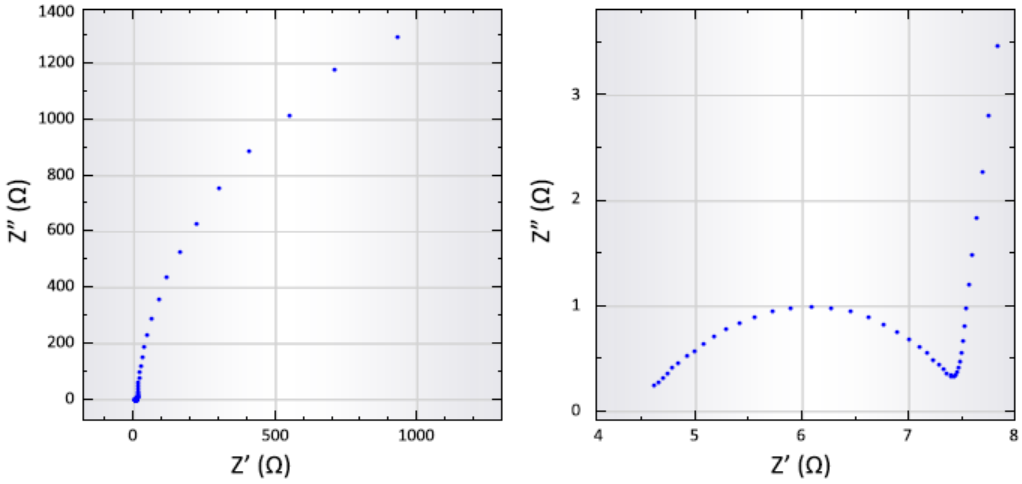

Figure 7. Nyquist plot for CNT-O_2 electrode *versus* Ag/AgCl in H_2SO_4 (0.5 M). To the right, detail of high frequency regions.

Impedance behavior shows two processes occurring in high and low frequencies. In the first region there is a well-established behavior for high frequencies, where we can observe the presence of a semi-circle related to the processes of charge transfer in the electrode. From the adjustment to this region, the electrolyte resistance was estimated to be 4.52 **Ω**; the charge transfer resistance was 3.08 **Ω** and the double layer capacitance was 8.34 µF.

The high value of the electrolyte resistance indicates there might be an additional resistive component contributing to this parameter. Since this value is much more superior than expected to the resistivity of the H_2SO_4 0.5 M electrolyte we suppose that the contact between the CNT-O_2 film and the metallic substrate imposes this resistance. Charge transfer resistance was also greater than expected, revealing that the interaction between the working electrode and electrolyte can be improved. It can reflect the fact that this particular sample was functionalized for 1 minute, resulting in an inferior hydrophilic character than those who suffered treatment for 2 minutes. This is also observed by the low value of the double layer capacitance.

The second region of the Nyquist plot refers to the system answer to low frequencies disturbances. It can confirm the capacitive behavior of the CNT-O_2 film, where the imaginary part of the impedance increases drastically to lower frequencies. There's an increasing influence of diffusion processes in lower frequencies, leading to the conclusion that when frequency is reduced there is enough time for the interaction to occur on the electrode most intern pores, depending on a slow diffusion process.

Since only the functionalized part of the CNT contributes to capacitance, and the plasma functionalization does not modify the CNT completely (only the exposed tube tips), it is suggested that the actual capacitance could be higher than calculated if we considerate only the CNT mass that effectively contributes for the formation of electrical double layer. This is corroborated by Shah *et al*. (2009), who show that specific capacitance of CNT-based supercapacitors increases with decrease of tube length.

Ervin *et al*. (2012) have commented in their work that one disadvantage of using multi-walled nanotubes is that the innermost walls contribute to the mass but not to the film surface area. Raul *et al*. (2012) reinforce this affirmation with their work, in which it was observed that specific capacitance for CNT increases with decreasing of diameter and the spacing of internal tubes.

4. CONCLUSIONS

The natural superhydrophobic character of carbon nanotubes can restrict its applications, but this situation can be remedied by the oxygen plasma functionalization, which turns it to superhydrophilic. This functionalization is a permanent modification of the film surface, allowing it to be widely studied by the electrochemical field. Control over the functionalization process is a key point for tuning the wettability ideally.

The investigation of electrochemical properties showed that the CNT-O_2/Ti-6Al-4V electrode has reasonable specific capacitance; it is comparable to other studies found in the literature and it has shown us where it can be improved (control over tube length as well as the addition of oxygen-containing groups and the diffusion barrier between Ti alloy and CNT film).

Nanoparticles such as CNT have the potential to greatly improve storage systems such as batteries and capacitors, especially due to the many modifications they can benefit from.

5. ACKNOWLEDGEMENTS

The authors gratefully acknowledge CNPq for financial support and LAS/INPE and UNIVAP for collaboration.

6. REFERENCES

Aleixo, L. M., 2003. "Voltametria: conceitos e técnicas". *www.chemkeys.com*, Vol. 52, p. 104. Available at <http://chemkeys.com/br/2003/03/25/voltametria-conceitos-e-tecnicas/>. Acessed on 10 oct. 2017.

Bird, J., 2010. *Electrical and Electronic Principles and Technology*. Elsevier Limited, 427 p.

Chen, J. H., Li, W. Z., Wang, D. Z., Yang, S. X., Wen, J. G., Ren, Z. F., 2002. "Electrochemical characterization of carbon nanotubes as electrode in electrochemical double-layer capacitors". *Carbon*, Vol. 40, p. 1193.

Chen, W., Fan, Z., Gu, L., Bao, X., Wang, C., 2010. "Enhanced capacitance of manganese oxide via confinement inside carbon nanotubes". *Chemical Communications*, Vol. 46, n. 22, p. 3905.

Costa, S., Borowiak-Palen, E., Kruszyñska, M., Bachmatiuk, A., Kaleńczuk, R. J., 2008. "Characterization of carbon nanotubes by Raman spectroscopy". *Material Science of Poland*, Vol. 26, n. 2, p. 433.

Cui, X., Hu, F., Wei, W., Chen, W., 2011. "Dense and long carbon nanotube arrays decorated with Mn_3O_4 nanoparticles for electrodes of electrochemical supercapacitors". *Carbon*, Vol. 49, p. 1225.

Ervin, M. H., Mailly, B., Palacios, T., 2012. "A comparison of single-wall carbon nanotube electrochemical capacitor electrode fabrication methods". *Electrochimica Acta*, Vol. 65, p. 37.

Etacheri, V., Marom, R., Elazari, R., Salitra, G., Aurbach, D., 2011. "Challenges in the development of advanced Li-ion batteries: a review". *Energy & Environmental Science*, Vol. 4, p. 3243.

Guittet, M. E., 2011. *Vertically aligned carbon nanotubes for supercapacitor and the effect of surface functionalization to its performance*. Master thesis, Ecole Polytechnique Federale de Lausanne, Lausanne.

Kim, B., Chung, H., Min, B. K., Kim, H., Kim, W., 2010. "Electrochemical capacitors based on aligned carbon nanotubes directly synthesized on tantalum substrates". *Bulletin of the Korean Chemical Society*, Vol. 31, n. 12, p. 3697.

Li, Y., Chen, C., 2017. "Polyaniline/carbon nanotubes-decorated activated carbon fiber felt as high-performance, free-standing and flexible supercapacitor electrodes". *Journal of Materials Science*, Vol. 52, n. 20, p. 12348.

Moraes, F. C. Silva, T. A., Cesarino, I., Machado, S. A. S., 2013. "Effect of the surface organization with carbon nanotubes on the electrochemical detection of bisphenol A". *Sensors and Actuators B: Chemical*, Vol. 177, p. 14.

Niu, Z., Zhou, W., Chen, J., Feng, G., Li, H., Ma, W., Li, J., Dong, H., Ren, Y., Zhao, D., Xie, S., 2011. "Compact-designed supercapacitors using free-standing single-walled carbon nanotube films". *Energy & Environmental Science*, Vol. 4, p. 1440.

Oliveira, P. C. A., Bertazzoli, R., 2011. "Determinação da densidade de corrente de corrosão em meios de baixa condutividade: uso de microeletrodos para minimizar a queda ôhmica". *Química Nova*, Vol. 34, n. 2, p. 325.

Osswald, S., Flahaut, E., Ye, Y., Gogotsi, Y., 2005. "Elimination of d-band in Raman spectra of doublewall carbon nanotubes by oxidation". *Chemical Physics Letters*, Vol. 402, p. 422.

Punbusayakul, N., 2012. "Carbon nanotubes architectures in electroanalysis". *Procedia Engineering*, Vol. 32, p. 683.

Rao, A., Jorio, A., Pimenta, M., Dantas, M., Saito, R., Dresselhaus, G., Dresselhaus, M., 2000. "Polarized raman study of aligned multiwalled carbon nanotubes". *Physical Review Letters*, Vol. 84, p. 1820.

Shah, R., Zhang, X. F., Talapatra, S., 2009. "Electrochemical double layer capacitor electrodes using aligned carbon nanotubes grown directly on metals". *Nanotechnology*, Vol. 20, n. 39, p. 395202.

Silva, T. A. Zanin, H., Saito, E., Medeiros, R. A., Vicentini, F. C., Corat, E. J., Fatibello-Filho, O., 2014. "Electrochemical behavior of vertically aligned carbon nanotubes and graphene oxide nanocomposite as electrode material". *Electrochimica Acta*, Vol. 119, p. 114.

Simon, P., Burke, A., 2008. "Nanostructured carbons: double layer capacitance and more". *The Electrochemical Society's Interface*, p. 38.

Simon, P., Gogotsi, Y., 2008. "Materials for electrochemical capacitors". *Nature Materials*, Vol. 7, p. 845.

Wei, S., Kang, W. P., Davidson, J. L., Huang, J. H., 2008. "Supercapacitive behavior of CVD carbon nanotubes grown on Ti coated Si wafer". **Diamond and Related Materials**, Vol. 17, p. 906.

Zanin, H., Saito, E., Ceragioli, H. J., Baranauskas, V., Corat, E. J., 2014. "Reduced graphene oxide and vertically aligned carbon nanotubes superhydrophilic films for supercapacitors devices". *Materials Research Bulletin*, Vol. 49, p. 487.

Zoski, C. G., 2007. *Handbook of Electrochemistry*. Elsevier Science.

7. RESPONSIBILITY NOTICE

The authors are the only responsible for the printed material included in this paper.